

# Identifying non-Abelian topological ordered state and transition by momentum polarization

Yi Zhang and Xiao-Liang Qi

Department of Physics, Stanford University, Stanford, California 94305, USA

(Dated: February 28, 2022)

Using a method called momentum polarization, we study the quasiparticle topological spin and edge-state chiral central charge of non-Abelian topological ordered states described by Gutzwiller-projected wave functions. Our results verify that the fractional Chern insulator state obtained by Gutzwiller projection of two partons in bands of Chern number 2 is described by  $SU(2)_2$  Chern-Simons theory coupled to fermions, rather than the pure  $SU(2)_2$  Chern-Simons theory. In addition, by introducing an adiabatic deformation between one Chern number 2 band and two Chern number 1 bands, we show that the topological order in the Gutzwiller-projected state does not always agree with the expectation of topological field theory. Even if the parton mean-field state is adiabatically deformed, the Gutzwiller projection can introduce a topological phase transition between Abelian and non-Abelian topologically ordered states. Our approach applies to more general topologically ordered states described by Gutzwiller-projected wave functions.

## I. INTRODUCTION

Topologically ordered states (TOSs) are unconventional states of matter with ground-state degeneracy, elementary quasiparticle excitations with fractional statistics, and long-range quantum entanglement<sup>1</sup>. The non-Abelian TOSs are a subcategory of TOSs in which quasiparticles carry nonlocal topological degeneracy and have received much recent attention due to their potential applications in topological quantum computations<sup>2-4</sup>. The braiding processes of quasiparticles within a non-Abelian TO induce noncommuting unitary transformations in the ground-state space instead of merely incurring a  $U(1)$  phase factor as in the Abelian case. Candidates for non-Abelian TOSs include the  $\nu = 5/2$  and  $\nu = 12/5$  fractional quantum Hall states<sup>5</sup>, which are proposed to be the Moore-Read state<sup>6</sup> and the Read-Rezayi states<sup>7</sup>.

Unlike conventional states of matter characterized by the symmetries preserved or those broken spontaneously, TOSs are characterized by topological properties such as ground-state degeneracy and fusion and braiding of topological quasiparticles. Except for some exactly solvable models, most candidate systems for TOSs can be studied only by numerical methods such as the density-matrix renormalization group (DMRG)<sup>8</sup> and the variational Monte Carlo method<sup>9</sup>. To determine the topological order in a numerically studied system, it is essential to develop numerical probes of topological properties. The search for more efficient and general numerical methods has attracted much recent attention. Various methods have been developed to characterize quasiparticle statistics based on direct calculation of the Berry phase<sup>1</sup>, explicit braiding of excitations<sup>10</sup> and modular transformation of ground states with minimum entanglement entropy<sup>11</sup>. Recently, an additional approach has been proposed for numerically extracting two topological properties of a given TOS, the topological spins of quasiparticles  $h_a$  and the edge-state chiral central charge  $c$ <sup>12</sup>. Physically, the topological spin determines the phase factor  $\theta_a = e^{i2\pi h_a}$  obtained by the system when a quasiparticle spins through  $2\pi$ . The chiral central charge of the edge state determines the thermal current  $I_E = \frac{c}{6}T^2$  at temperature  $T$ <sup>13</sup>. These two quantities are essential in determining the TOS. The proposal is based on the concept of

*momentum polarization* defined for cylindrical systems. For a cylindrical lattice system with periodic boundary condition along the  $y$  direction, one can define a unitary “partial translation operator”  $T_y^L$  which translates the lattice sites along the  $y$  direction by one lattice constant for all sites that are in the left half of the system. For a topological ground state  $|\Phi_a\rangle$  with quasiparticle type  $a$  in the cylinder, the expectation value of  $T_y^L$  is proposed to have the following asymptotic form<sup>12</sup>

$$\lambda_a \equiv \langle \Phi_a | T_y^L | \Phi_a \rangle \simeq \exp \left[ \frac{2\pi i}{L_y} p_a - \alpha L_y \right] \quad (1)$$

where  $L_y$  is the number of lattice sites in the  $\hat{y}$  direction,  $\alpha$  is a nonuniversal complex constant for the leading contribution and independent of the specific topological sector  $a$ , and remarkably, the fractional part of the momentum polarization  $p_a$  has a universal value  $p_a = h_a - \frac{c}{24}$ , which measures the combination of topological spin  $h_a$  (modulo 1) and central charge  $c$  (modulo 24). Since  $T_y^L$  only acts only on the left half of the system, the momentum polarization is a quantum entanglement property determined by the reduced density matrix of the left half of the system. The average value  $\lambda_a$  has the merit of being relatively simple to evaluate in comparison with the previous methods based on entanglement entropy<sup>11</sup>. The calculation of the Renyi entanglement entropy involves a swap operator and requires a minimum of two replicas of the system, while for momentum polarization the evaluation of  $T_y^L$  does not need a replica so the Hilbert space for Monte Carlo sampling is much smaller for the same system size. In Ref. 12, the momentum polarization was studied for two simple TOSs, the Laughlin  $1/2$  state in fractional Chern insulators (the definition of which will be given in the next paragraph) and the honeycomb lattice Kitaev model<sup>14</sup>. The former is an Abelian state, while the latter has a special non-Abelian state that can be solved by mapping to free Majorana fermions.

In this paper, we apply the momentum polarization approach to more generic non-Abelian TOSs. More specifically, we study non-Abelian states described by Gutzwiller-projected wave functions<sup>15</sup> of fractional Chern insulators (FCIs). An (integer) Chern insulator is a band insulator with nonzero quantized Hall conductance. The Hall conductance  $\sigma_H = n \frac{e^2}{h}$  carried by an occupied band is determined by a

topological invariant of the energy band, known as the Chern number  $C = n$ . FCIs are generalizations of Chern insulators to interacting systems, which have fractional Hall conductance and topological order. One way to understand FCIs is through the parton construction, in which the electron is considered as a composite particle of several “partons” carrying fractional quantum numbers. For example, an electron can be split into three fermionic partons, with each parton in an integer Chern insulator with  $C = 1$ . The corresponding electron state has Hall conductance  $\frac{1}{3}\frac{e^2}{h}$  and is the  $\frac{1}{3}$  Laughlin state. Gauge fields are coupled to partons to enforce the constraint that all physical states are electron states and no individual parton will be observed. The parton construction can be expressed in ansatz ground state wave functions constructed by the procedure of Gutzwiller projection<sup>15</sup>, which is a projection of the parton ground state into the physical electron Hilbert space. Gutzwiller-projected wave functions have been constructed for FCI<sup>16</sup>. When two partons are glued together to form a bosonic “electron”, and each parton is in a state with Chern number  $C = 1$ , from topological effective field theory (which we will review later in the paper) one expects to find a  $1/2$  bosonic Laughlin state. In contrast, if each parton is in a state with Chern number  $C = 2$ , the resulting electron TOS is expected to be non-Abelian, related to  $SU(2)$  level-2 Chern-Simons (CS) theory<sup>6</sup>. The non-Abelian nature of this state has been verified by calculation of the modular  $S$  matrix for the projected wave functions<sup>17</sup>.

In this paper, we study the momentum polarization of the Gutzwiller-projected wave function for the state of two partons with Chern number  $C = 2$ . In addition to confirming the non-Abelian topological order of this state, our result contains the following two points. First, the spin and central charge obtained from momentum polarization clearly distinguish two related but distinct topological states, the  $SU(2)_2$  CS theory and the  $SU(2)_2$  CS theory coupled to fermions<sup>18</sup>. The particle fusion, braiding, and modular  $S$  matrix of these two theories are identical, but they are distinct TOSs with different edge-state chiral central charge  $c = \frac{3}{2}$  and  $c = \frac{5}{2}$ , respectively. The momentum polarization calculation clearly demonstrates that the Gutzwiller-projected parton wave function has the topological order of the latter theory. Second, there is an apparent paradox in the statement that Gutzwiller projection of parton  $C = 2$  states leads to  $SU(2)_2$  CS theory coupled to fermions. Since Chern number is the only topological invariant of a fermion energy band, a Chern number  $C = 2$  band can be adiabatically deformed to two decoupled  $C = 1$  bands, as long as translation symmetry breaking is allowed. Since the Gutzwiller projection of two  $C = 1$  partons is known to give the Laughlin  $1/2$  state, it appears that one can adiabatically deform the non-Abelian TOS obtained from partons occupying the  $C = 2$  band to the Abelian TOS of two decoupled Laughlin  $1/2$  states. This is clearly in contradiction with the topological stability of TOSs. By introducing an explicit adiabatic deformation between a  $C = 2$  band structure and two decoupled  $C = 1$  bands, we study the quasiparticle topological spin during the adiabatic interpolation. Our result shows that there is a topological phase transition between the Abelian phase of the bilayer Laughlin state and the non-Abelian phase

of the  $SU(2)_2$  CS coupled to fermions. The topological phase transition occurs at a *finite* coupling between the two  $C = 1$  bands. In other words, the TOS obtained from Gutzwiller projection of  $C = 2$  parton bands is *not* completely determined by the Chern number of the parton band structure, but may depend on details of the Chern bands and the projection. The argument based on parton “mean-field theory”, *i.e.*, integrating over partons to obtain CS gauge theory, may not predict the correct phase. This example further emphasizes the importance of numerical approaches such as momentum polarization in identifying TOSs. Based on this numerical observation, we will also discuss theoretically the effective theory interpretation of this topological phase transition.

The remaining of the paper is organized as follows: In Sec. II, we present our momentum polarization calculation in the Gutzwiller-projected wave function of non-Abelian FCIs, after reviewing the relevant background knowledge. Sec. II A presents our projective construction and the  $C = 2$  Chern insulator model; Sec. II B gives a brief field theory discussion of the corresponding TOS; Sec. II C shows our numerical results from momentum polarization. We obtain the topological spin of the non-Abelian quasiparticle  $h_\sigma = 0.321 \pm 0.013$  and the fermion quasiparticle  $h_\psi = 0.520 \pm 0.026$  and edge central charge  $c = 2.870 \pm 0.176$ , in agreement with the  $SU(2)$  CS theory coupled to fermions ( $h_\sigma = 5/16$  and  $c = 5/2$ ). In Sec. III, we introduce the adiabatic deformation between two  $C = 1$  bands and one  $C = 2$  band, and study the topological phase transition between the two TOSs. In Sec. III A, we present an adiabatic interpolation of the parton tight-binding Hamiltonian. Sec. III B presents the results for the quasiparticle topological spin and ground-state degeneracy which indicate the transition between the non-Abelian and Abelian TOS; In Sec. III C, we discuss the physical interpretation of this topological transition. Finally, Sec IV is devoted to a conclusion from our main results and discussion of open questions.

## II. IDENTIFYING THE NON-ABELIAN TOS IN $C = 2$ FCI

### A. The projective construction and $C = 2$ Chern insulator model

The projective construction is a powerful formalism for ansatz wave functions of many TOS<sup>19</sup>. For our projective construction, we first introduce several species of partons  $\psi_a$  as free fermions in a Chern insulator, and then constrain the partons to recombine into physical “electrons” (which may be bosons or fermions). In the simple Gutzwiller-projected states we will discuss in this work, the projected wave function is defined in first quantized language by  $\Phi(\{z_i\}) = \prod_a \psi_a(\{z_i\})$ . Here  $\{z_i\}$  with  $i = 1, 2, \dots, N$  are the coordinates of all particles, and  $\psi_a(\{z_i\})$  is the wave function of the  $a$ -th parton.  $N$  is the number of each parton type, which is the same as the total electron number of the system. The properties of the resulting states can be numerically computed through variational Monte Carlo calculations.

For our focused non-Abelian TOS, we start with the following parton mean-field Hamiltonian on a two-dimensional

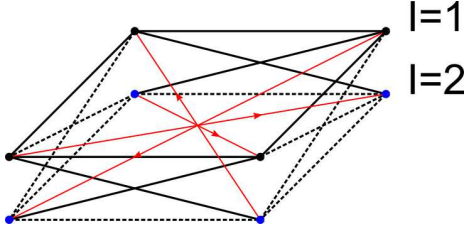


FIG. 1: An illustration of the hopping Hamiltonian in Eq. 2. The two orbitals on each lattice site are shown as different layers and colored in black and blue, respectively. The hopping is +1 (−1) along the solid (dashed) lines, and  $i/\sqrt{2}$  (− $i/\sqrt{2}$ ) along (against) the red arrows.

square lattice

$$\begin{aligned}
 H_{C=2} &= \sum_{\langle ij \rangle, I, s} (-1)^{I-1} c_{jI s}^\dagger c_{iI s} + \sum_{\langle ij \rangle, s} e^{i2\theta_{ij}} (c_{j2s}^\dagger c_{i1s} + c_{j1s}^\dagger c_{i2s}) \\
 &+ \frac{1}{\sqrt{2}} \sum_{\langle\langle ik \rangle\rangle, s} e^{i2\theta_{ik}} (c_{k2s}^\dagger c_{i1s} - c_{k1s}^\dagger c_{i2s}) + \text{H.C.} \\
 &= \sum_{\langle ij \rangle_x, s} [(c_{j1s}^\dagger c_{i1s} - c_{j2s}^\dagger c_{i2s}) - (c_{j2s}^\dagger c_{i1s} + c_{j1s}^\dagger c_{i2s})] \\
 &+ \sum_{\langle ij \rangle_y, s} [(c_{j1s}^\dagger c_{i1s} - c_{j2s}^\dagger c_{i2s}) + (c_{j2s}^\dagger c_{i1s} + c_{j1s}^\dagger c_{i2s})] \\
 &+ \frac{1}{\sqrt{2}} \sum_{\langle\langle ik \rangle\rangle, s} e^{i2\theta_{ik}} (c_{k2s}^\dagger c_{i1s} - c_{k1s}^\dagger c_{i2s}) + \text{H.C.} \quad (2)
 \end{aligned}$$

where  $I = 1, 2$  are the two orbitals on each lattice site and  $s = \uparrow, \downarrow$  labels the two flavors of partons.  $\theta_{ij}$  is the azimuthal angle for the vector connecting  $i$  and  $j$ .  $\langle ij \rangle$  and  $\langle\langle ik \rangle\rangle$  label nearest neighbor and next nearest neighbor links, while  $\langle ij \rangle_x$  and  $\langle ij \rangle_y$  denote nearest neighbors along the  $\hat{x}$  and  $\hat{y}$  directions, respectively, as is illustrated in Fig. 1. A previous study<sup>17</sup> has shown that at half filling the system is a Chern insulator with  $C = 2$ . The correlation length  $\xi$  is on the order of a lattice constant, and therefore the finite-size effects are generally suppressed for the system sizes we study.

In real space, the parton wave function  $\psi_a(\{z_i\})$  is a Slater determinant for a completely filled valence band, where  $z = (i, I)$  labels both the position and orbital indices of a parton. Next we apply the Gutzwiller projection imposing the constraint  $n_{i\uparrow} = n_{i\downarrow}$ , with  $n_{iI s} = c_{iI s}^\dagger c_{iI s}$  the number of partons at each site and orbital. The states satisfying this constraint have two partons bound at each site and orbital, and are physical electron states with electron number  $n_{iI}^e = n_{i\uparrow}$ . This leads to the following many-body wave function

$$\Phi(\{z_i\}) = \psi_\uparrow(\{z_i\}) \psi_\downarrow(\{z_i\}) = \psi_\uparrow^2(\{z_i\}) \quad (3)$$

This state is the major focus of the paper. Previously, the three topological sectors on a torus for this projective construction were obtained by tuning the boundary condition of the parton mean-field Hamiltonian in Eq. 2 and their connection to the corresponding threaded quasiparticle has been established<sup>17</sup>. For our momentum polarization calculations,

we need to generalize the projective construction to a cylinder. To resolve the complication from the gapless chiral edge modes on the open edges, we start from a torus and adiabatically lower all hopping amplitudes across the open boundary until they are much smaller than the edge modes' finite size gap. The residue hoppings effectively couple only the zero energy states at  $k_y = \pm\pi/2$  on the two edges of the cylinder, therefore the original boundary conditions of topological sectors on the torus lead to linear combinations of the zero energy states<sup>12</sup>. Since such a process involves no level crossing, we can obtain the topological sectors on a cylinder by allowing occupation of different parton zero-energy states on the two edges.

## B. Topological Field Theory Description

To understand the TOS described by the above projective construction, we briefly review the topological field theory description of this state. The electron operator can be expressed in partons as  $f_{iI} = c_{iI\uparrow} c_{iI\downarrow}$ . This decomposition has an  $SU(2)$  gauge symmetry: for any  $SU(2)$  matrix with  $\alpha, \beta \in \mathbb{C}$  and  $|\alpha|^2 + |\beta|^2 = 1$

$$\begin{pmatrix} c_{iI\uparrow} \\ c_{iI\downarrow} \end{pmatrix} \rightarrow \begin{pmatrix} \alpha & \beta \\ -\beta^* & \alpha^* \end{pmatrix} \begin{pmatrix} c_{iI\uparrow} \\ c_{iI\downarrow} \end{pmatrix} \quad (4)$$

this transformation preserves the electron operator  $f_{iI} \rightarrow (\alpha c_{iI\uparrow} + \beta c_{iI\downarrow})(-\beta^* c_{iI\uparrow} + \alpha^* c_{iI\downarrow}) = c_{iI\uparrow} c_{iI\downarrow} = f_{iI}$ , and therefore the effective theory of partons should also be gauge invariant. The simplest possible effective theory satisfying the gauge invariant condition is obtained by a minimal coupling of the mean-field Hamiltonian (2) to an  $SU(2)$  gauge field<sup>20</sup>. A lattice  $SU(2)$  gauge field is described by gauge connection  $e^{ia_{ij}} \in SU(2)$  defined along each link  $ij$ . The Hamiltonian is written as

$$\begin{aligned}
 H_{eff} &= \sum_{\langle ij \rangle, I} (-1)^{I-1} e^{ia_{ij}^{II}} c_{jI s}^\dagger c_{iI s} + \sum_{\langle ij \rangle} e^{i2\theta_{ij}} e^{ia_{ij}^{II}} (c_{j2s}^\dagger c_{i1s} + c_{j1s}^\dagger c_{i2s}) \\
 &+ \frac{1}{\sqrt{2}} \sum_{\langle\langle ik \rangle\rangle} e^{i2\theta_{ik}} e^{ia_{ik}^{II}} (c_{k2s}^\dagger c_{i1s} - c_{k1s}^\dagger c_{i2s}) + \text{H.C.} \quad (5)
 \end{aligned}$$

where  $s, r = \uparrow, \downarrow$  denote the two parton species, and repeated indices are summed over.

Since the partons are gapped, it is straightforward to integrate them out. Due to the Chern number  $C = 2$  of each parton band, integrating over the parton results in an  $SU(2)_2$  non-Abelian CS theory

$$\mathcal{L} = \frac{2}{4\pi} \epsilon_{\mu\nu\rho} \text{tr} \left[ a_\mu \partial_\nu a_\rho + \frac{2}{3} a_\mu a_\nu a_\rho \right] \quad (6)$$

However, it is not accurate to say that the topological field theory describing the TOS of this parton construction is  $SU(2)_2$  CS gauge theory, because the partons have non-trivial contribution to topological properties such as edge theory. The edge theory of  $SU(2)_2$  CS theory is a chiral  $SU(2)_2$  Weiss-Zumino-Witten (WZW) model<sup>21,22</sup>, while the edge theory of the FCI described above consists of four chiral fermions

	$SU(2)_2$ CS	$\nu = 2$ coupled to $SU(2)_2$
$c$	3/2	5/2
$h_1$	0	0
$h_\sigma$	3/16	5/16
$h_\psi$	1/2	1/2
$D$	3	3

TABLE I: Theoretical values of topological properties including the edge central charge  $c$ , the topological spins for quasiparticles  $h_1$ ,  $h_\sigma$ ,  $h_\psi$  and the ground-state degeneracy  $D$  for the pure  $SU(2)_2$  CS theory and the  $\nu = 2$  fermions coupled to an  $SU(2)_2$  gauge field (or equivalently, the  $\frac{U(4)_1}{SU(2)_2}$  theory).

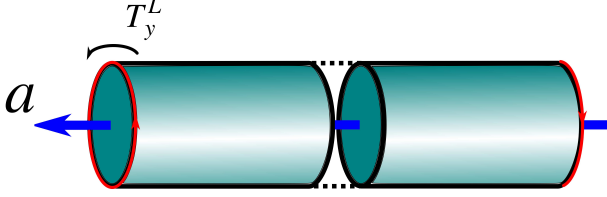


FIG. 2: The partial translation operator  $T_y^L$  translates the left half of the cylinder by one lattice constant along the  $\hat{y}$  direction. The red arrows indicate the chiral edge modes. The topological sector  $a$  is determined by the type of quasiparticle threaded through the cylinder, denoted by the large blue arrow.

(two from each flavor of parton) coupled to the  $SU(2)_2$  WZW model. Technically, the edge state of fermions coupled to the WZW model is described by a quotient of two conformal field theories  $\frac{U(4)_1}{SU(2)_2}$ , in which  $U(4)_1$  describes four free chiral fermions and  $SU(2)_2$  describes the gauge degrees of freedom which are removed from physical excitations.<sup>18</sup> Although they both have three quasiparticles with the same fusion rule and braiding statistics, these two theories are not topologically equivalent. In particular, the topological spin differs by a fermionic sign for quasiparticles which correspond to an odd number of holes in the parton Chern insulator state. For comparison purpose, we list the theoretical values for the quasiparticle topological spins and edge central charges for the two theories in Table I.

In summary, we have seen that the effective topological field theory analysis suggests that the topological order in the Gutzwiller-projected state is  $\frac{U(4)_1}{SU(2)_2}$  instead of  $SU(2)_2$ . However, it is essential to verify that directly for the Gutzwiller-projected wave function, as there is no guarantee that the effect of Gutzwiller projection is completely equivalent to the coupling to a gauge field in the effective field theory. This is achieved in the next section by studying the momentum polarization.

### C. Topological spin and edge central charge from momentum polarization calculations

Quasiparticle braiding from previous studies has determined that the TOS for  $\Phi(\{z_i\})$  is necessarily non-Abelian.

However, both theories in Table 1 are consistent with the braiding, and therefore additional information is necessary to make a complete identification. We numerically extract the quasiparticle topological spin and edge central charge from momentum polarization calculations for the model in Eq. 2 defined on a cylinder.

Care should be taken about the non-Abelian topological sector, which consists of parton states with an overall difference of momentum  $\pi$  on the left edge. For the expectation value of the partial translation operator  $T_y^L$  that translates the left half of the cylinder by one lattice constant along the  $\hat{y}$  direction, see Fig. 2 for illustration, this  $\pi$  momentum difference will result in contributions with opposite signs. To overcome this difficulty, we generalize  $T_y^L$  to twist the left half of the cylinder by  $l$  lattice constants, so that the overall phase difference vanishes for a partial translation of  $l = 2$  lattice constants. For this purpose, we take  $\frac{L_y}{l}$  to be integer, consider  $l$  sites along the  $\hat{y}$  direction as one unit cell, and replace  $L_y$  by  $\frac{L_y}{l}$  in the formula proposed in Ref. 12. Consequently, the average value of  $T_y^L$  defined by  $\lambda_a = \langle \Phi_a | T_y^L | \Phi_a \rangle$  has the following leading contributions

$$\lambda_a = \exp \left[ i \frac{2\pi l}{L_y} p_a - \alpha \frac{L_y}{l} \right] \quad (7)$$

in which  $\alpha$  is a nonuniversal complex constant independent of the specific topological sector  $a$ , while  $p_a$  has a universal topological value  $p_a = h_a - c/24$  determined by the topological spin  $h_a$  and the edge central charge  $c$ .

The quantity in Eq. 7 can be efficiently evaluated for the projected wave functions with the variational Monte Carlo method. For a cylinder with  $L_x = 8$ ,  $L_y = 16$  and  $T_y^L$  translating the left half by  $l = 2$  lattice constants for the aforementioned reason, numerical calculations yield  $\arg(\lambda_1) = -3.4449 \pm 0.0063$  for the identity sector,  $\arg(\lambda_\sigma) = -3.1929 \pm 0.0082$  for the sector associated with the non-Abelian quasiparticle, and  $\arg(\lambda_\psi) = -3.0366 \pm 0.0257$  for the fermion sector. With  $h_1 = 0$  by definition of the identity particle, we obtain

$$h_\sigma = \frac{L_y}{2\pi l} [\arg(\lambda_\sigma) - \arg(\lambda_1)] = 0.321 \pm 0.013 \quad (8)$$

$$h_\psi = \frac{L_y}{2\pi l} [\arg(\lambda_\psi) - \arg(\lambda_1)] = 0.520 \pm 0.026 \quad (9)$$

This is fully consistent with the theoretical value of  $h_\sigma^{th} = 5/16 = 0.3125$  for the non-Abelian quasiparticle and  $h_\psi^{th} = 1/2 = 0.5$  for the fermion quasiparticle of a theory of  $\nu = 2$  fermions couple to an  $SU(2)$  gauge field.

In addition, we calculate  $\lambda_1$  for  $L_x = 8$ ,  $l = 1$ , and various values of  $L_y$ . The numerical results are shown in Fig. 3. To compare with Eq. 7, note that  $-L_y \arg(\lambda_1) = \text{Im} \alpha L_y^2 - 2\pi p_1$ , so the intercept of this linear fitting gives the value of  $-2\pi p_1 = 2\pi c/24 = 0.7513 \pm 0.046$ . The resulting value of  $c = 2.870 \pm 0.176$  is also fairly consistent with the prediction of  $c^{th} = 5/2$  according to the theory of  $\nu = 2$  fermions coupled to an  $SU(2)$  gauge field. Although there is a deviation between the numerical value and the theoretical value  $5/2$  which is probably due to the finite-size effect, the



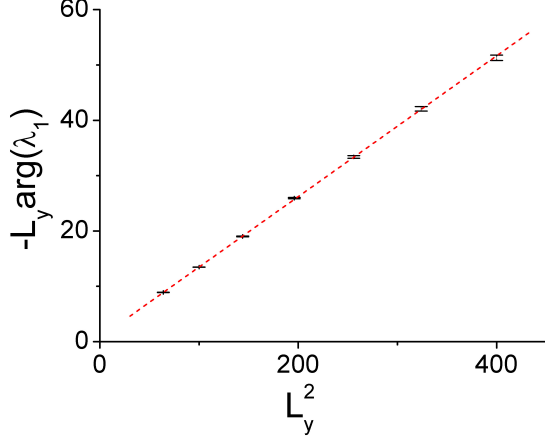


FIG. 3: The value of  $-L_y \arg(\lambda_1)$  versus  $L_y^2$  for the identity sector  $a = 1$ . The intercept at  $L_y^2 = 0$  of the linear fitting gives  $-2\pi p_1 = 0.7513 \pm 0.046$ . We set  $L_x = 8$  and  $l = 1$  for all calculations.

accuracy of the result is sufficient to completely distinguish this system from the bare  $SU(2)_2$  CS theory with  $h_\sigma = 3/16$  and  $c = 3/2$ . This result also provides further evidence that the momentum polarization method for computing topological quantities is applicable to non-Abelian TOSs.

### III. THE TRANSITION BETWEEN ABELIAN AND NON-ABELIAN TOS IN PROJECTED WAVE FUNCTIONS

From the results discussed in the last section, it seems that the TOS of the Gutzwiller-projected wave function agrees well with the expectation from the topological field theory approach. However, there is a hidden paradox in this result. Since the Chern number is the only topological invariant for a generic energy band in two dimensions, a band with Chern number  $C = 2$  is topologically equivalent to two  $C = 1$  bands. More explicitly, an exact mapping has been constructed between a  $C = 2$  band and two decoupled Landau level systems which are related by a lattice translation operation<sup>23–25</sup>. Therefore one would naively expect that a state with each parton in a  $C = 2$  Chern insulator is adiabatically equivalent to one in which each parton occupies two  $C = 1$  bands. However, this statement seems to contradict the fact that the Gutzwiller-projected wave function of the latter state is Abelian. It is known that the Gutzwiller-projected wave function of two partons each in a  $C = 1$  band gives a Laughlin  $\nu = \frac{1}{2}$  Abelian TOS<sup>11,12,16,26–28</sup>, which is also denoted  $SU(2)_1$  Chern-Simons theory. Therefore one would expect that when each parton occupies two decoupled  $C = 1$  bands, which can be viewed as two decoupled layers, the Gutzwiller-projected wave function of the whole system is simply two copies of the Laughlin  $\nu = \frac{1}{2}$  state, *i.e.*  $SU(2)_1 \times SU(2)_1$ , which is an Abelian state clearly distinct from the  $\frac{U(4)}{SU(2)_2}$  theory we ob-

tained earlier from both effective theory and numerical results. To resolve this apparent paradox, in this section we introduce an explicit interpolation between the  $C = 2$  model used in last section and a model with two decoupled  $C = 1$  bands. By studying the momentum polarization of the corresponding Gutzwiller-projected wave functions during this interpolation, we find a topological phase transition between the Abelian and non-Abelian phases.

#### A. An adiabatic interpolation of the parent Hamiltonian

As an explicit example of the interpolation between a  $C = 2$  band and two  $C = 1$  bands, we consider the following parton mean-field Hamiltonian on a two-dimensional square lattice<sup>29</sup>

$$H_\Theta = \sqrt{2} \sum_{\langle ij \rangle_{y,s}} \left[ \cos \Theta (c_{j1s}^\dagger c_{i1s} - c_{j2s}^\dagger c_{i2s}) - \sin \Theta (c_{j2s}^\dagger c_{i1s} + c_{j1s}^\dagger c_{i2s}) \right] \\ + \sqrt{2} \sum_{\langle ij \rangle_{x,s}} \left[ \sin \Theta (c_{j1s}^\dagger c_{i1s} - c_{j2s}^\dagger c_{i2s}) + \cos \Theta (c_{j2s}^\dagger c_{i1s} + c_{j1s}^\dagger c_{i2s}) \right] \\ + \frac{1}{\sqrt{2}} \sum_{\langle\langle ik \rangle\rangle_{s}} e^{i2\theta_{ik}} (c_{k2s}^\dagger c_{i1s} - c_{k1s}^\dagger c_{i2s}) + \text{H.C.} \quad (10)$$

where the label definition is the same as in Eq. 2, and  $\Theta$  is a continuous parameter. For  $\Theta = \pi/4$ , Eq. 10 returns to the Hamiltonian in Eq. 2 with a  $C = 2$  band. For  $\Theta = 0$ , the Hamiltonian becomes

$$H_{\Theta=0} = \sqrt{2} \sum_{\langle ij \rangle_{y,s}} (c_{j1s}^\dagger c_{i1s} - c_{j2s}^\dagger c_{i2s}) + \sqrt{2} \sum_{\langle ij \rangle_{x,s}} (c_{j2s}^\dagger c_{i1s} + c_{j1s}^\dagger c_{i2s}) \\ + \frac{1}{\sqrt{2}} \sum_{\langle\langle ik \rangle\rangle_{s}} e^{i2\theta_{ik}} (c_{k2s}^\dagger c_{i1s} - c_{k1s}^\dagger c_{i2s}) + \text{H.C.} \quad (11)$$

The hopping matrix elements are drawn in Fig. 4. Since hoppings exist only between  $I = 1 (I = 2)$  orbitals on the  $x_i$  odd sites and  $I = 2 (I = 1)$  orbitals on the  $x_i$  even sites, the system can be directly decomposed into two uncoupled subsystems with even and odd values of  $x_i + I$ . The two subsystems are related by a translation by one lattice constant along the  $\hat{x}$  direction. Suppressing the orbital index, each of the two subsystems has the following Hamiltonian, which is a Chern insulator with  $C = 1$  for each parton flavor  $s$

$$H_{C=1} = \sum_{\langle ij \rangle, s} t_{i,j} c_{is}^\dagger c_{js} + \sum_{\langle\langle ik \rangle\rangle, s} \Delta_{i,k} c_{is}^\dagger c_{ks} + \text{H.C.} \quad (12)$$

where the nearest neighbor hopping amplitude  $t_{i,j}$  is  $\sqrt{2}$  along the  $\hat{x}$  direction and alternates between  $\sqrt{2}$  and  $-\sqrt{2}$  along the  $\hat{y}$  direction, and the next nearest neighbor is  $\Delta_{i,k} = i/\sqrt{2}$  along the arrow and  $\Delta_{i,k} = -i/\sqrt{2}$  against the arrow, see Fig. 5 for an illustration. The unit cell contains two lattice sites. Therefore, Eq. 10 defines an interpolation between one Chern insulator with  $C = 2$  and two decoupled Chern insulators each with  $C = 1$ .

It is also verified that the interpolation is adiabatic and the band gap remains finite for all  $\Theta$ . Actually, the Hamiltonians

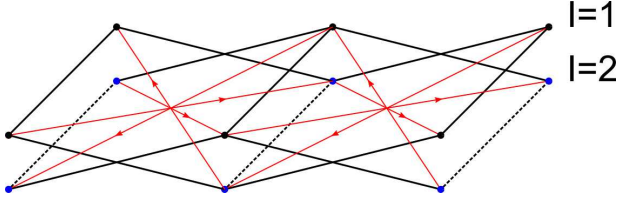


FIG. 4: An illustration of the hopping Hamiltonian in Eq. 11. The two orbitals on each lattice site are shown in different layers and colored in black and blue, respectively. The hoppings along the solid (dashed) lines are  $+\sqrt{2}$  ( $-\sqrt{2}$ ), and along (against) the red arrows are  $i/\sqrt{2}$  ( $-i/\sqrt{2}$ ). It is straightforward to separate the system into two uncoupled zigzag subsystems with odd and even values of  $x_i + l$ .

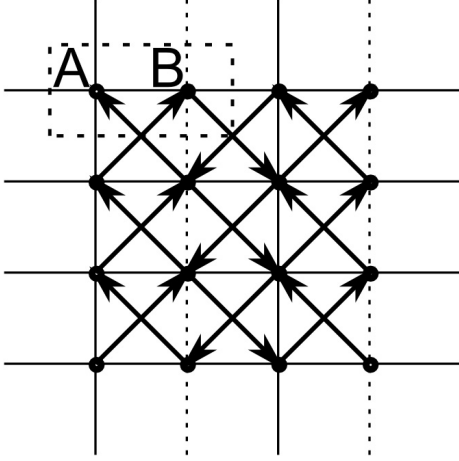


FIG. 5: Illustration of a  $C = 1$  Chern insulator model on a two-dimensional square lattice. The nearest neighbor hopping amplitudes are  $\sqrt{2}$  along the square edges and  $-\sqrt{2}$  along the dashed lines. The next nearest neighbor hoppings are along the square diagonal with amplitude  $+i/\sqrt{2}$  along  $(-i/\sqrt{2})$  against the arrow. The two lattice sites in the unit cell are marked as A and B.

with different  $\Theta$  can be related by a global unitary transformation on the orbital space

$$H_\Theta = U^{-1} H_0 U$$

$$U = \exp \sum_s \left[ \frac{\Theta}{2} (c_{i1s}^\dagger c_{i2s} - c_{i2s}^\dagger c_{i1s}) \right] \quad (13)$$

The effect of the rotation on annihilation operators is

$$U^{-1} \begin{pmatrix} c_{i1s} \\ c_{i2s} \end{pmatrix} U = \begin{pmatrix} \cos \frac{\Theta}{2} & -\sin \frac{\Theta}{2} \\ \sin \frac{\Theta}{2} & \cos \frac{\Theta}{2} \end{pmatrix} \begin{pmatrix} c_{i1s} \\ c_{i2s} \end{pmatrix} \quad (14)$$

Consequently, the dispersion and band gap are intact with respect to the variation of  $\Theta$ .

Now we study the Gutzwiller-projected state corresponding to the parton mean-field Hamiltonian  $H_\Theta$ . We have shown that  $H_{\Theta=\frac{\pi}{4}}$  leads to the  $\frac{U(4)_1}{SU(2)_2}$  state. On the other hand,  $H_{\Theta=0}$  describes two decoupled “layers”, each with two partons in  $C = 1$  bands. The Gutzwiller projection also applies separately to the two layers, so that the resulting state is a decoupled bilayer of the projected  $C = 1$  states. The projected wave

	$SU(2)_1 \times SU(2)_1$ CS	$\nu = 2$ coupled to $SU(2)_2$
$c$	2	5/2
$D$	4	3
$h$	0, 1/4, 1/4, 1/2	0, 5/16, 1/2

TABLE II: Theoretical values of topological properties including the edge central charge  $c$ , ground-state degeneracy  $D$ , and quasiparticle topological spins for the  $SU(2)_1 \times SU(2)_1$  CS theory and the  $\nu = 2$  fermions coupled to an  $SU(2)_2$  gauge field.

functions from a Chern insulator with  $C = 1$  have been confirmed to be consistent with the  $SU(2)_1$  CS theory<sup>11,12,16,26–28</sup>. Correspondingly, the projected wave function of two uncoupled Chern insulators each with  $C = 1$  should be describable by an Abelian  $SU(2)_1 \times SU(2)_1$  CS theory, which has four Abelian particles and is clearly distinct from the non-Abelian TOS established for  $\Theta = \frac{\pi}{4}$ . There are major differences in their topological properties including the torus ground-state degeneracy, edge central charge and quasiparticle topological spins, as listed in Table II. Due to this topological difference between  $\Theta = 0$  and  $\Theta = \frac{\pi}{4}$ , a topological phase transition must occur for some intermediate  $\Theta$ . Since the parton ground states before Gutzwiller projection with different  $\Theta$  are related by a local unitary transformation, one has to conclude that the topological phase transition is introduced by the Gutzwiller projection procedure. We study this topological phase transition numerically in the next section.

### B. The quasiparticle topological spin as a signature for topological phase transition

First of all, we would like to determine whether there is a first-order phase transition at some  $\Theta$ . Even though the interpolation of the parton ground state before projection is clearly adiabatic, the same is not necessarily true for the projected wave function. Numerically, for  $H_\Theta$  defined on a system of size  $L_x = L_y = 12$  with periodic boundary conditions, we study the evolution of the projected wave functions with steps of  $\Theta$  as small as  $\delta\Theta = \frac{\pi}{400}$ . Variational Monte Carlo calculations<sup>16</sup> indicate that for all values of  $\Theta \in [0, \frac{\pi}{4}]$ , the overlap between neighboring steps’ wave functions  $|\langle \Phi(\Theta + \delta\Theta) | \Phi(\Theta) \rangle| = 1 - O(10^{-3})$ , which clearly suggests that  $\langle \delta\Phi(\Theta) | \Phi(\Theta) \rangle \rightarrow 0$  for small  $\delta\Theta \rightarrow 0$  and excludes the presence of singularities. Therefore the quantum phase transition must be continuous.

In particular, the open boundary conditions are equivalent for the semion sector in the Abelian TOS and the non-Abelian quasiparticle sector in the non-Abelian TOSs, as well as for the identity sectors in both TOS, making an adiabatic interpolation possible within each sector. To determine the topological phase transition point, we compute the momentum polarization with  $l = 2$  for the identity and semion (non-Abelian quasiparticle) sectors of the projected wave functions on a cylinder of  $L_x = 8$  and  $L_y = 12$ , 16 for each interpolation of Eq. 10. The results of topological spin  $h$  for the semion (non-

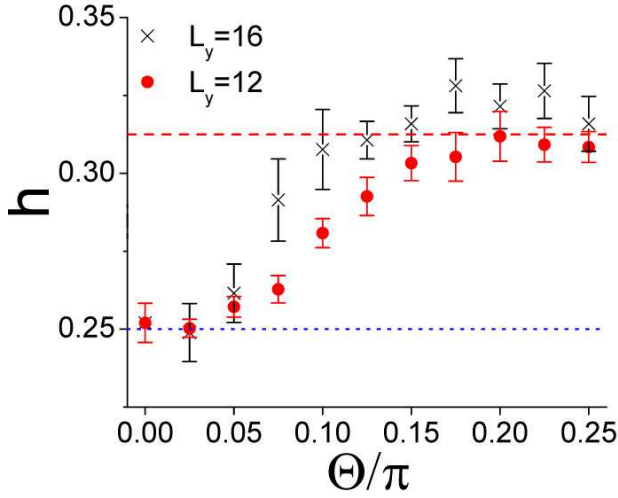


FIG. 6: The topological spin  $h$  for the semion (non-Abelian quasiparticle) sector versus various values of  $\Theta \in [0, \pi/4]$  for the projected Chern insulator in Eq. 10 from momentum polarization calculations. The red dashed line and the blue dotted line are the theoretical values of  $h$  for the  $SU(2)_1 \times SU(2)_1$  CS theory ( $h_s = 1/4$ ) and  $\nu = 2$  fermions coupled to an  $SU(2)$  gauge field ( $h_\sigma = 5/16$ ), respectively.

Abelian quasiparticle) sector versus  $\Theta \in [0, \pi/4]$  are shown in Fig. 6. For small value of  $\Theta = 0.05\pi$ , the topological spin starts to deviate from the semionic statistics of  $h_s = 1/4$  for the Abelian TOS and evolve towards  $h_\sigma = 5/16$  for the non-Abelian TOS, see Table II. Still, there is a finite region of  $\Theta$  where the value of  $h$  represents an Abelian TOS. For further verification, for a smaller value of  $\Theta = 0.025\pi$ , we numerically calculated the overlaps between projected wave functions of various boundary conditions on an  $L_x = L_y = 12$  torus<sup>16</sup> and find that there are four linearly independent candidate ground-state wave functions by projective construction, consistent with the Abelian  $SU(2)_1 \times SU(2)_1$  CS theory. In contrast, for values such as  $\Theta = \pi/4$  and  $\Theta = 3\pi/8$  fully in the parameter region of the non-Abelian topological order, such linear independence is only three fold.

Our numerical results show that a topological phase transition occurs at finite  $\Theta$ , which is consistent with the fact that the  $\Theta = 0$  Abelian state is topologically stable and should persist for a finite region of  $\Theta$ : the fractional Chern insulator is an intrinsic topological ordered state protected by an excitation gap that is stable against small local perturbations of arbitrary form such as weak couplings between the subsystems. Since the two subsystems are coupled for all nonzero  $\Theta$ , the mean-field Hamiltonian at nonzero  $\Theta$  can be viewed only as a Chern insulator with a  $C = 2$  band. Therefore the topological field theory approach will predict that the TOS of the system is described by  $SU(2)_2$  Chern-Simons theory coupled to  $C = 2$  partons, as we discussed in Sec. II. In contrast, our numerical result for small  $\Theta$  finds an Abelian TOS, which provides a concrete example of a case when the TOS of the Gutzwiller-projected wave function is different from the prediction of topological field theory.

### C. Theoretical interpretation of the topological phase transition

To understand physically the topological phase transition, we first ask why the derivation of the effective field theory in Sec II B does not apply to  $\Theta = 0$ . For general  $\Theta$ , the constraints on the partons induces an  $SU(2)$  gauge field along all lattice edges in Fig. 1 that dominates the low-energy theory after the partons are integrated out. In the  $\Theta = 0$  limit, however, the Hamiltonian becomes Eq. 11, and all hoppings between the two subsystems vanish. Therefore there are two well-defined  $SU(2)$  gauge fields in the long wavelength limit, one for each subsystem. As is clear in Fig. 4, these two  $SU(2)$  gauge fields exist on independent pieces and remain independent after the partons are integrated out. Integrating out the  $C = 1$  band of the parton gives the  $SU(2)$  level 1 Chern-Simons theory, so that the topological field theory of the  $\Theta = 0$  system consists of fermions coupling to  $SU(2)_1 \times SU(2)_1$ .

At finite  $\Theta$ , coupling is turned on between the two effective “layers” and breaks the separate  $SU(2) \times SU(2)$  gauge symmetry into one single  $SU(2)$ . As an alternative view of the symmetry breaking, one can carry out the unitary rotation in Eq. 13 in reverse to transform the Hamiltonian  $H_\Theta$  back to  $H_0$ . In the new basis, the partons occupy the two decoupled  $C = 1$  bands before projection. The only way the two independent layers are coupled is through the constraint. In the original basis the constraint is written as  $n_{i\uparrow} = n_{i\downarrow}$  ( $c_{i\uparrow}^\dagger c_{i\uparrow} = c_{i\downarrow}^\dagger c_{i\downarrow}$ ) in real space. After the inverse unitary transformation for a finite  $\Theta$ , the resulting constraints are  $c_{i1\uparrow}^\dagger c_{i1\uparrow} + c_{i1\downarrow}^\dagger c_{i1\downarrow} = c_{i1\downarrow}^\dagger c_{i1\downarrow} + c_{i1\uparrow}^\dagger c_{i1\uparrow}$  and  $\cos \Theta (c_{i1\uparrow}^\dagger c_{i1\uparrow} - c_{i1\downarrow}^\dagger c_{i1\downarrow}) + \sin \Theta (c_{i2\uparrow}^\dagger c_{i2\uparrow} + c_{i2\downarrow}^\dagger c_{i2\downarrow}) = \cos \Theta (c_{i1\downarrow}^\dagger c_{i1\downarrow} - c_{i1\uparrow}^\dagger c_{i1\uparrow}) + \sin \Theta (c_{i2\downarrow}^\dagger c_{i2\downarrow} + c_{i2\uparrow}^\dagger c_{i2\uparrow})$ . The latter explicitly breaks the intra-layer charge conservation symmetry of the parent Hamiltonian in Eq. 11, defined by  $c_{i\uparrow}^\dagger \rightarrow e^{-i\phi} c_{i\uparrow}^\dagger$ ,  $c_{i\downarrow} \rightarrow e^{i\phi} c_{i\downarrow}$ ,  $x_i + I \in \text{odd}$ . As a consequence of this inter-layer coupling, the two  $SU(2)$  gauge fields in the effective theory are coupled and only a diagonal  $SU(2)$  gauge symmetry is preserved. Physically, the holes in the two  $C = 1$  bands are no longer distinguishable so that the two semionic quasiparticles originating from the holes in the two bands now merge to one particle. Consequently, the ground-state degeneracy on a torus, effectively labeled by the quasiparticle content, also decreases from four fold to three fold.

The discussion above suggests that the Abelian and non-Abelian phases are distinguished by whether the two layers (in the rotated parton basis) have separately conserved particle numbers. In the Abelian (non-Abelian) phase, the separate particle number conservation of the two layers is effective (broken). To verify this scenario, we numerically calculate the fluctuations of parton number in one of the  $C = 1$  layers (in the rotated parton basis):  $N_1 = \sum_{I+x_i \in \text{odd}} c_{i\uparrow}^\dagger c_{i\uparrow}$ . In the  $\Theta = 0$  limit, the two bands are independent, therefore  $N_1 = \bar{N}_1$  and the fluctuation is exactly zero. As  $\Theta$  increases, the intra-band charge conservation is broken, and therefore one may expect an increase in the  $N_1$  fluctuation. Fig. 7 is a histogram of the number of sampled configurations in the

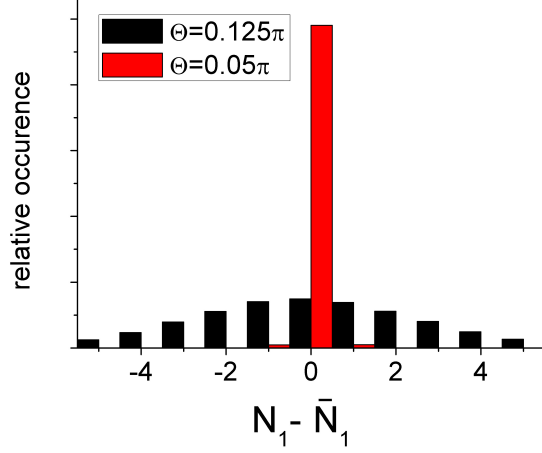


FIG. 7: A histogram of the number of sampled configurations versus the parton number around its average  $N_1 - \bar{N}_1$  in one of the decomposed  $C = 1$  bands. While the  $N_1 = \bar{N}_1$  central peak contains more than 98% of the configurations for  $\Theta = 0.05\pi$  (red), the spread for  $\Theta = 0.125\pi$  (black) is much wider and the percentage of the  $N_1 = \bar{N}_1$  configurations is only 15% suggesting that  $N_1$  is no longer a good quantum number. The results are obtained on system size  $L_x = L_y = 28$  with periodic boundary conditions.

projected wave function versus the parton number  $N_1$  fluctuation around its average value  $\bar{N}_1$  in one of the  $C = 1$  bands at  $\Theta = \pi/20$  (red) and  $\Theta = \pi/8$  (black). While such fluctuation is still largely suppressed and the  $N_1$  conservation approximately holds at  $\Theta = \pi/20$  on the Abelian TOS side of the transition, it proliferates at  $\Theta = \pi/8$  and the intralayer charge conservation no longer exists for a non-Abelian TOS. To see further the connection between the parton number fluctuation and the non-Abelian TOS, we show in Fig. 8 the mean squared deviation  $\sqrt{\langle (N_1 - \bar{N}_1)^2 \rangle} / \bar{N}_1$  versus  $\Theta$  for various system sizes.

In reality, for a multiband TOS such as the topological nematic states<sup>24</sup>, band mixing, be it hopping or interaction, is hard to eliminate. The existence of a finite  $\Theta_c$  suggests that the Abelian TOS is stable against weak band-mixing perturbations. Intuitively, this is because the TOS are protected by excitation gaps. For small band-mixing perturbations, the charge conservation within the bands can appear as an emergent symmetry. Nevertheless, in comparison with integer Chern insulators protected by the band gap, the TOS are relatively vulnerable. A topological phase transition can occur even if the band structure remains adiabatically equivalent.

#### IV. CONCLUSIONS

In conclusion, we study topological properties of non-Abelian TOS using Gutzwiller-projected wave functions and the momentum polarization approach. Our numerical results on the topological spin and edge central charge confirm that

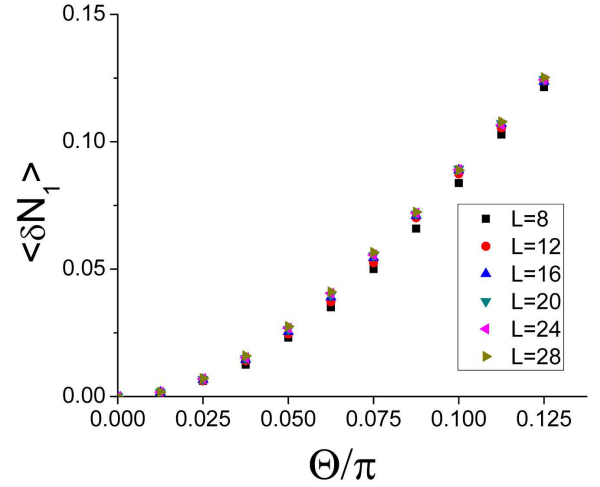


FIG. 8: The mean squared deviation  $\sqrt{\langle (N_1 - \bar{N}_1)^2 \rangle} / \bar{N}_1$  versus  $\Theta$  for system sizes  $L_x = L_y = 8, 12, 16, 20, 24, 28$ .

projected wave functions of two partons in Chern bands with Chern number  $C = 2$  are described by the field theory of  $\nu = 2$  fermions coupled to an  $SU(2)$  gauge field, and clearly distinguish it from the pure  $SU(2)_2$  CS theory. In addition, we adiabatically interpolate the parent Chern insulator with  $C = 2$  with two Chern insulators each with  $C = 1$ , and track the variation of topological quantities such as the topological spin and ground-state degeneracy for their corresponding TOS projected wave functions. We show that the topological phase transition between the non-Abelian and Abelian TOS is marked by the breaking down of charge conservation within each of the  $C = 1$  Chern bands. The transition point is close to but apart from the completely decoupled limit, in consistency with the intuition that the corresponding Abelian TOS is protected by a gap and stable against small band-mixing perturbations. Our result demonstrates explicitly that the topological order in a Gutzwiller-projected state does not always agree with the prediction of topological field theory, and generically has to be determined by numerical calculations of topological properties.

Our numerical methods based on momentum polarization and the variational Monte Carlo method are generalizable to more complicated non-Abelian TOSs described by Gutzwiller-projected wave functions. Compared to previous approaches, momentum polarization provides an efficient way to extract characteristic quantities given the many-body wave functions of a chiral topological ordered state. One open question left for future work is whether the critical behavior of momentum polarization across a topological phase transition can be studied numerically and compared with any field theory description. Another open question is whether there is a more generic proof of the momentum polarization formula in Eq. 7, which has been verified numerically in several TOS, but has not been proved analytically except for arguments based on edge-state conformal field theory<sup>12</sup>.

We would like to thank Maissam Barkeshli, Chao-Ming



Jian, Ching Hua Lee and Peng Ye for insightful discussions. This work is supported by the Stanford Institute for The-

oretical Physics (YZ) and the National Science Foundation through the grant No. DMR-1151786 (XLQ).

- 
- <sup>1</sup> X.-G. Wen, Int. J. Mod. Phys. B **4**, 239 (1990).
  - <sup>2</sup> E. Dennis, A. Kitaev, A. Landahl, and J. Preskill, Journal of Mathematical Physics **43**, 4452 (2002).
  - <sup>3</sup> A. Kitaev, Annals of Physics **303**, 2 (2003).
  - <sup>4</sup> C. Nayak, S. H. Simon, A. Stern, M. Freedman, and S. Das Sarma, Rev. Mod. Phys. **80**, 1083 (2008).
  - <sup>5</sup> R. Willett, J. P. Eisenstein, H. L. Störmer, D. C. Tsui, A. C. Gos-sard, and J. H. English, Phys. Rev. Lett. **59**, 1776 (1987).
  - <sup>6</sup> G. Moore and N. Read, Nuclear Physics B **360**, 362 (1991).
  - <sup>7</sup> N. Read and E. Rezayi, Phys. Rev. B **59**, 8084 (1999).
  - <sup>8</sup> H.-C. Jiang, Z. Wang, and L. Balents, Nat Phys **8**, 902 (2012).
  - <sup>9</sup> X.-G. Wen, Phys. Rev. B **65**, 165113 (2002).
  - <sup>10</sup> F. A. Bais and J. C. Romers, New Journal of Physics **14**, 035024 (2012).
  - <sup>11</sup> Y. Zhang, T. Grover, A. Turner, M. Oshikawa, and A. Vishwanath, Phys. Rev. B **85**, 235151 (2012).
  - <sup>12</sup> H.-H. Tu, Y. Zhang, and X.-L. Qi, Phys. Rev. B **88**, 195412 (2013).
  - <sup>13</sup> I. Affleck, Phys. Rev. Lett. **56**, 746 (1986).
  - <sup>14</sup> A. Kitaev, Annals of Physics **321**, 2 (2006).
  - <sup>15</sup> C. Gros, Annals of Physics **189**, 53 (1989).
  - <sup>16</sup> Y. Zhang, T. Grover, and A. Vishwanath, Phys. Rev. B **84**, 075128 (2011).
  - <sup>17</sup> Y. Zhang and A. Vishwanath, Phys. Rev. B **87**, 161113 (2013).
  - <sup>18</sup> M. Barkeshli and X.-G. Wen, Phys. Rev. B **81**, 155302 (2010).
  - <sup>19</sup> X. G. Wen, Phys. Rev. Lett. **66**, 802 (1991).
  - <sup>20</sup> X.-G. Wen, Phys. Rev. B **60**, 8827 (1999).
  - <sup>21</sup> J. Wess and B. Zumino, Physics Letters B **37**, 95 (1971).
  - <sup>22</sup> E. Witten, Nuclear Physics B **223**, 422 (1983).
  - <sup>23</sup> X.-L. Qi, Physical review letters **107**, 126803 (2011).
  - <sup>24</sup> M. Barkeshli and X.-L. Qi, Phys. Rev. X **2**, 031013 (2012).
  - <sup>25</sup> Y.-L. Wu, N. Regnault, and B. A. Bernevig, Physical review letters **110**, 106802 (2013).
  - <sup>26</sup> V. Kalmeyer and R. B. Laughlin, Phys. Rev. Lett. **59**, 2095 (1987).
  - <sup>27</sup> V. Kalmeyer and R. B. Laughlin, Phys. Rev. B **39**, 11879 (1989).
  - <sup>28</sup> X. G. Wen, F. Wilczek, and A. Zee, Phys. Rev. B **39**, 11413 (1989).
  - <sup>29</sup> C. H. Lee and X.-L. Qi, arXiv preprint arXiv:1308.6831 (2013).